Research Article

Flood Susceptibility Analysis in the West Rapti River Basin Using Frequency Ratio Model

Tek Narayan Bhattarai[1,2,3], Swastik Ghimire[1,4,*]

[1]   Department of Civil Engineering, Pulchowk Campus, Institute of Engineering, Tribhuvan University, Pulchowk, Lalitpur 44700, Nepal
[2]   Faculty of Environmental Science, Technische Universität Dresden, Dresden, Germany
[3]   IHE Delft Institute for Water Education, Delft, The Netherlands
[4]   School of Sustainable Engineering and the Built Environment, Arizona State University, Tempe, Arizona, USA

*Correspondence

Swastik Ghimire

E-mail: *swastikg32@gmail.com*
ORCID ID: 0000-0003-2006-8312

Abstract: Floods are recognized as lethal natural events, which result in devastating natural and human losses. So, identifying flood susceptible zones is crucial to adopt necessary mitigation strategies beforehand. With the advent of GIS tools and modelling techniques, mapping of such zones has become easier and more precise; yet flood prone countries like Nepal have not been able to embrace such tools for flood risk management. With a compelling need to address this situation, this paper employs the Frequency Ratio model to analyze flood susceptibility in the West Rapti River Basin. The model, created with the help of 77 flood points and tested with 30 points to obtain 80.7% accuracy, maps the flood susceptibility zones in the area and identifies the lower Terai and settlement regions as high-risk areas. With the increasing threat of changing climate in the future, this study also propounds better preparation of flood inventory maps in the future for more precise susceptibility analysis models and better flood risk management.

1. Introduction

Floods are regarded as one of the most catastrophic natural calamities, impacting a large number of people globally, and severely affecting the environment and socio-economic systems (Rahmati et al., 2016). In Asia and Pacific regions, most flood events have been caused due to erratic monsoon precipitation patterns owing to changing climate. Among all natural disasters, floods, along with landslides, are reported to be the cause of more than 50% of the human casualties in South-Asian countries like Nepal, India, Sri Lanka, and Bangladesh (Pangali Sharma et al., 2019). Its severe effects have been particularly seen in the agricultural sector, which is the major economic contributor to these countries.

Flood control and its risk management system are necessary to minimize significant risks to people, environment, and infrastructure. Therefore, identifying flood susceptible zones and analyzing their vulnerability is a crucial task for early warning systems and emergency services in developing preventative and mitigation methods for flood events in the future (Samanta et al., 2018). Flood susceptibility maps are essential tools to spatially represent such zones. Geographic Information Systems (GIS) have made the identification of flooding zones easier, allowing development of flood susceptibility maps more precisely (Liuzzo et al., 2019).

Previously, several approaches and strategies have been established and examined to map flood susceptibility. GIS based methods along with remote sensing techniques were used for flood vulnerability analysis in: inaccessible regions of North Korea (Lim & Lee, 2017); Shangyou region of China (Wang et al., 2019) and Sunsari district of Nepal (Uddin & Shrestha, 2011). Other models based on techniques like decision tree, logistic regression, frequency ratio were commonly used (Al-Juaidi et al., 2018; Natarajan et al., 2021; Rahmati et al., 2016; Sun et al., 2011). Among them, frequency ratio model (FRM) has been widely used with other methodologies for mapping flood susceptibility.

Nepal is vulnerable to extreme flood events due to its fragile geology, complex topography, extreme climatic events, and seismic activities which are exacerbated by rapid and uncontrolled urbanization (Bhattarai et al., 2022; Yogacharya & Gautam, 2016). Because of this, frequency of flood events in Nepal has been increasing, as indicated by recent floods in Melamchi, Kailali, Illam and other parts of Nepal (IFRC, 2021). However, only a limited number of studies regarding flood disaster have been carried out in specific basins and watersheds of Nepal (Pangali Sharma et al., 2019). Moreover, flood susceptibility mapping has been carried out only on Bishnumati river, Kankai river and Ratu Khola using HEC-RAS tool (Dangol & Bormudoi, 2017; Karki et al., 2011; Shrestha, 2002).

The West Rapti River Basin (WRRB), located in the mid-western part of Nepal, is also susceptible to extreme flood events. The lower parts of WRRB have been inundated by flood each year due to heavy monsoon rainfall (about 80 % of the yearly precipitation) extending from June to September (Perera et al., 2015). Consequently, bank-cutting, erosion, and sedimentation have been persistently prevailing in the WRRB, which have further amplified the detrimental effects of flood events. However, detailed studies to identify flood risk zones in this basin have not been carried out, making flood risk management an arduous task. So, the purpose of this study is to map out the potential risk areas in the WRRB using FRM analysis. Further, with the increased uncertainty in

the variability of climatic parameters in the future, those risks may further be amplified and induce greater ramifications. Thus, the authors believe that the findings of this study may be useful to researchers, local governments, and policymakers in developing flood mitigation strategies by identifying high flood risk zones and applying necessary adaptation strategies to limit the negative repercussions elicited by extreme flood events by changing climate in the future. It also manifests a need for concerned authorities to promulgate disaster preparedness programs in high flood risk zones and consequently develop advanced measures like early warning systems in the future.

2. Study area

The WRRB lies in the mid-western region of Nepal (Figure 1). It extends from 27°56'50''N to 28°02'30" N latitude and 81°45'00" E longitude. The West Rapti River originates in Nepal's central highlands, flows through the plains, and eventually feeds into the Ghagra (Karnali) River, which is a tributary of the Ganges. It has a number of tributaries: Arun River, Jhimruk River, Dundhuwa River, Mari River, Lungri River, Sotiya, Sit River and Gandheli. The river flows downstream from the junction of the Jhimruk and Mari Rivers. The basin's average slope is 16.8%. The runoff is mainly caused by monsoon rainfall and groundwater and flow regimes are influenced by monsoon precipitation and groundwater. During non-monsoon times, groundwater flow helps in maintaining the minimum flow level, thus avoiding dryness (WEPA, 2011).

The upper WRRB has a temperate climate, whereas the lower basin, including the Banke region, has a tropical to subtropical climate. It is hot and dry from March to May; hot and humid from June to August; mild from September to October; and cold and cloudy with occasional showers due to westerly winds from November to February. The temperature in the lower area of the basin surpasses 46°C in the summer and falls below 2°C in the upper half of the basin during the winter. Summer monsoon rainfall falls in the study area from June to September, accounting for approximately 80% of total annual rainfall. The average rainfall is roughly 1500 mm. The relative humidity varies from roughly 60% in May to over 90% in January (Talchabhadel et al., 2015).
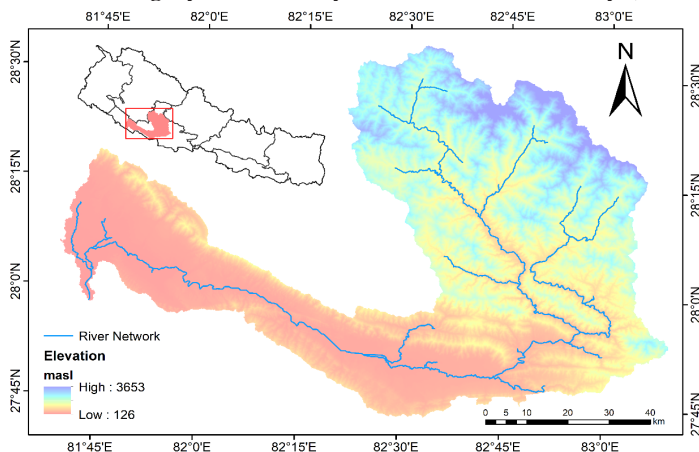

Figure 1. *Topography of West Rapti River Basin*

Data sources

The different data types used in this study are tabulated in Table 1 along with their sources. These data are analyzed using GIS software for various flood conditioning factors in order to map out high flood risk locations in the WRRB.

Table 1. Data sets used for flood susceptibility analysis

S.N.	Data Description	Purpose	Source	Resolution
1	SRTM DEM	Elevation, Slope, TWI	United States Geological Survey (USGS)	30 m
2	Soil	Soil texture map	Nepal Agricultural Research Council (NARC)	-
3	Lithology	Lithology map	USGS	-
4	Land Use	Land use map	Environment Systems and Research Institute (ESRI)	10m
5	Historic flood locations	Frequency Ratio Model	(Perera et al., 2015), Google earth topographic maps, Disaster Risk Management Portal (www.drrportal. gov.np)	Point
6	Rainfall Data	Rainfall distribution Map	Department of Hydrology and Meteorology	14 stations from 1980-2020 [Annex A]

3. Methodology

3.1 Flood inventory map

The likelihood of a flood event occurring in a given location in the future may be predicted by examining records of its past occurrences (Manandhar, 2010). So, flood inventory maps are crucial elements for the prediction of future floods. For the preparation of flood inventory map, past flood records from the Disaster Risk Management Portal (www.drrportal.gov.np), along with other relevant literatures in the area were thoroughly examined. The map (Figure 2), containing 107 flood locations was randomly characterized (Pradhan & Buchroithner, 2010) into two datasets, with about 70% (77) and 30% (30) locations adopted for training and testing respectively. To divide training and testing data, the random sampling method was used which is one of the oldest and most commonly used. The flood points are shuffled, and samples are chosen at random and placed in the train and test sets (Baheti, 2022).
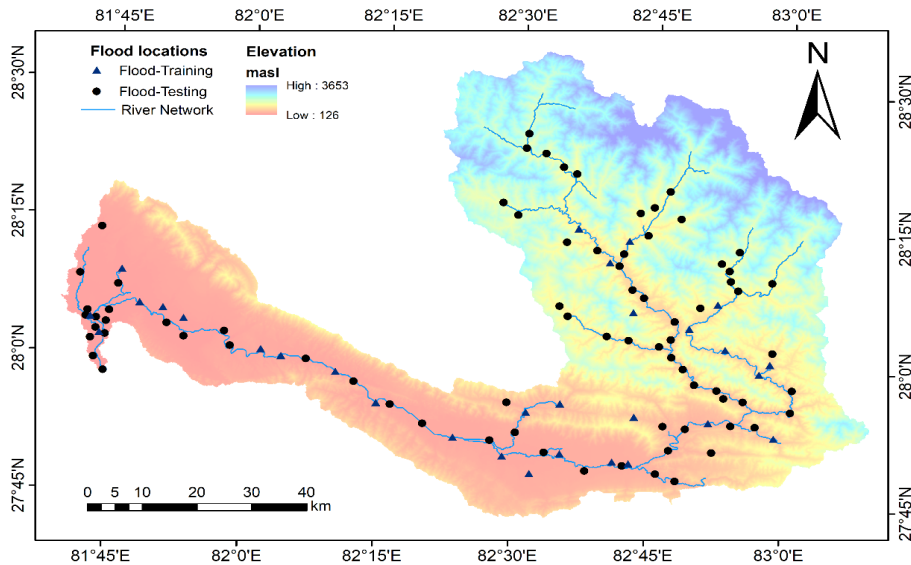
Figure 2. *Flood inventory map of WRRB*

3.2 Flood Conditioning Factors

In order to build flood susceptibility maps, it is important to identify the effective factors influencing flood occurrence (Kia et al., 2011). Thus, from literature review, eleven flood conditioning factors were selected, and these factors are briefly discussed in Table 2.

Table 2. *Description of flood conditioning factors*

Factors	Description	References
Lithology	Susceptibility to flood differs according to various lithological formations. The lithology of the basin determines its drainage and sediment output. In addition, the permeability of geological formations is critical in determining flood susceptibility. The data obtained from the USGS website was processed using the ArcGIS 10.5 to classify the lithological condition into 5 classes, as shown in Figure 3.	(Mario Denis et al., 2014)

Land use	The hydrological processes: infiltration, surface runoff, and evapotranspiration are all influenced by the land use. In the event of a flood, these mechanisms play a vital role. The data obtained from the ESRI website was processed using the ArcGIS 10.5 to classify the land use condition into 7 classes, as shown in Figure 4.	(Shafapour Tehrany et al., 2014)
Distance from river	The distance from the river is an important factor that influences flood spread and amplitude. The Euclidian distance tool in ArcGIS 10.5 was used to create the map, as shown in Figure 5.	(Glenn et al., 2012)
Soil Texture	The surface runoff, drainage, and flooding processes are controlled by the infiltration process, which is dependent on the texture of the soil. The data obtained from the NARC was processed using the ArcGIS 10.5 to classify soil texture into 7 classes, as shown in Figure 6.	(Cosby et al., 1984)
Slope angle	The slope angle governs surface runoff, infiltration, velocity of water and intensity of soil erosions. The runoff is slower in the gentle slope area, giving it more time to infiltrate. For preparing this map, 4 classes were separated using ArcGIS 10.5, as shown in Figure 7.	(Adiat et al., 2012)
Slope aspect	Slope aspect affects the soil moisture patterns and has a significant impact on hydrologic processes such as evapotranspiration and frontal precipitation direction, as well as weathering and plant development, especially in dry climates. The slope aspect map was also generated just like Slope Angle and classified into 9 classes, as shown in Figure 8.	(Ercanoglu & Gokceoglu, 2002)

| Plan curvature	Plan curvature can give the significant geomorphological information. In the case of plan curvature, negative curvature signifies concavity, zero curvature denotes flatness, and positive curvature denotes convexity. Using ArcGIS 10.5, 3 classes of plan curvature were created, as shown in Figure 9.	(Shafapour Tehrany et al., 2014)
Topographic Wetness Index (TWI)	TWI has a big influence on flood mapping as it governs the overland flow of water by describing the spatial distribution of wetness. It is calculated by using equation: $TWI = ln\left(\frac{a}{TanB}\right)$ Where, $a = \frac{Total\ basin\ area\ (A)}{Length\ of\ contour\ (L)}$ is the area of catchment and B is slope angle in degree. TWI map was created by processing DEM in the ArcGIS 10.5 using flow direction and raster calculator tool into 4 classes, as shown in Figure 10.	(Shafapour Tehrany et al., 2014)
Drainage Density	Drainage density is length of flow channels per unit area and has a great role in flood analysis. Using ArcGIS 10.5, 4 classes of drainage density were created, as shown in Figure 11.	(Onuşluel Gül, 2013)
Altitude	Different elevations have different soil texture, slope angle, slope aspect and other climatic characteristics. So, vulnerability of a particular region depends upon the altitude. Using ArcGIS 10.5, altitude was classified into 4 classes, as shown in Figure 12.	(Shafapour Tehrany et al., 2014)
Rainfall	Rainfall is often the main source of flood and often triggers flash flooding. 14 meteorological stations in and around the WRRB were selected and their normal annual rainfall based on periods 1980-2020 were calculated. Rainfall was classified into 4 classes using ArcGIS 10.5, as shown in Figure 13.	(Shafapour Tehrany et al., 2014)
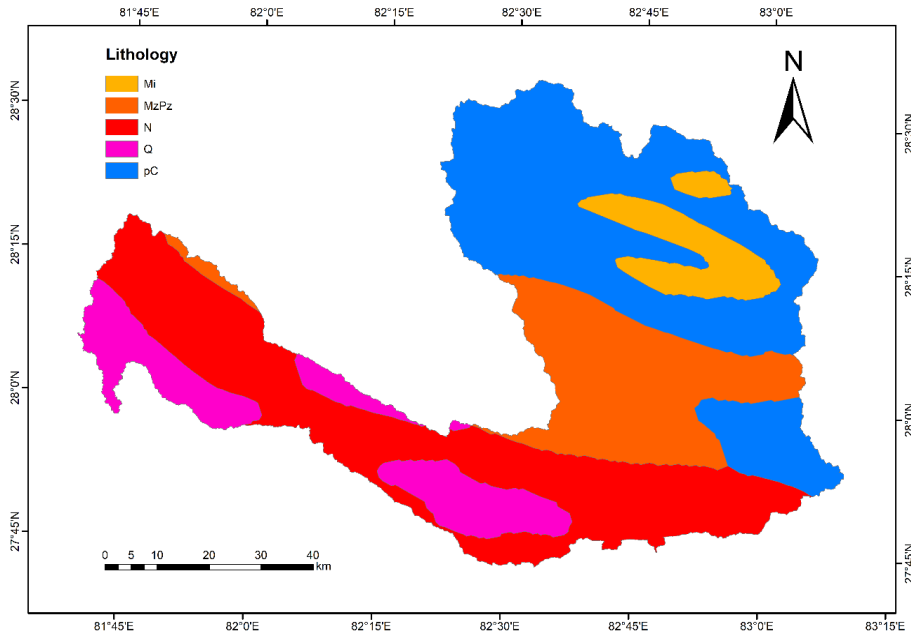
Figure 3. *Lithological map of WRRB*
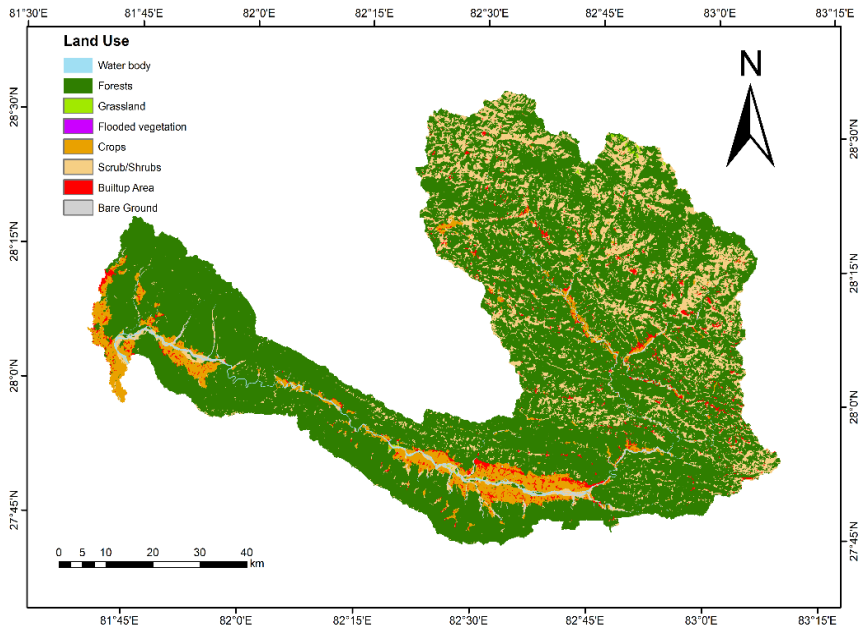
Figure 4. *Land use map*
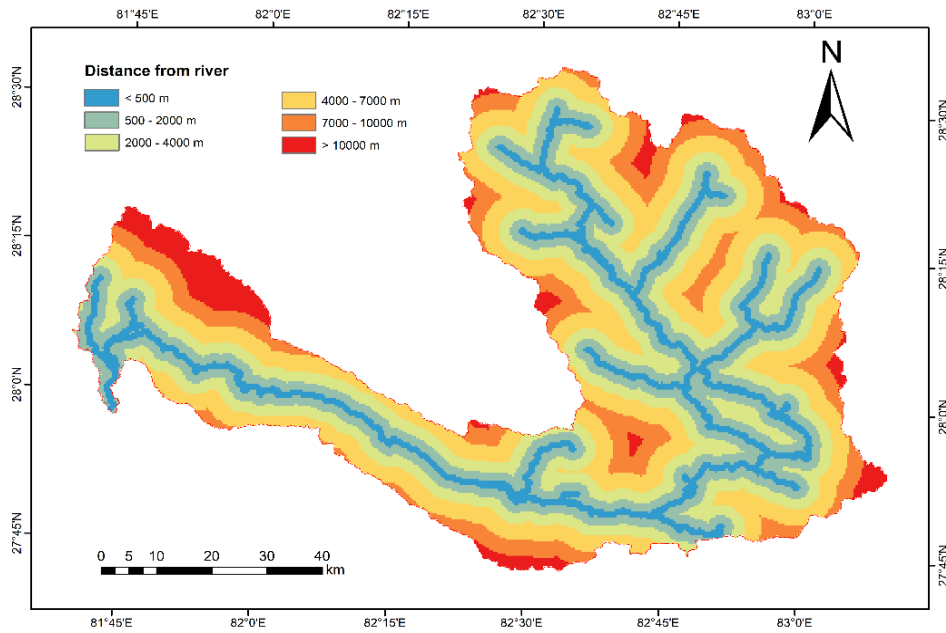
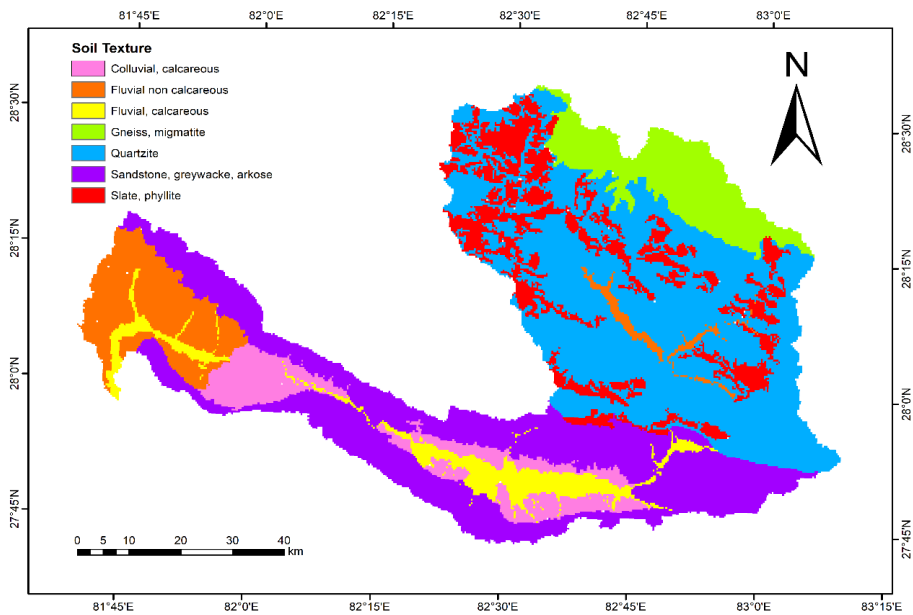**Figure 5.** *Distance from river*

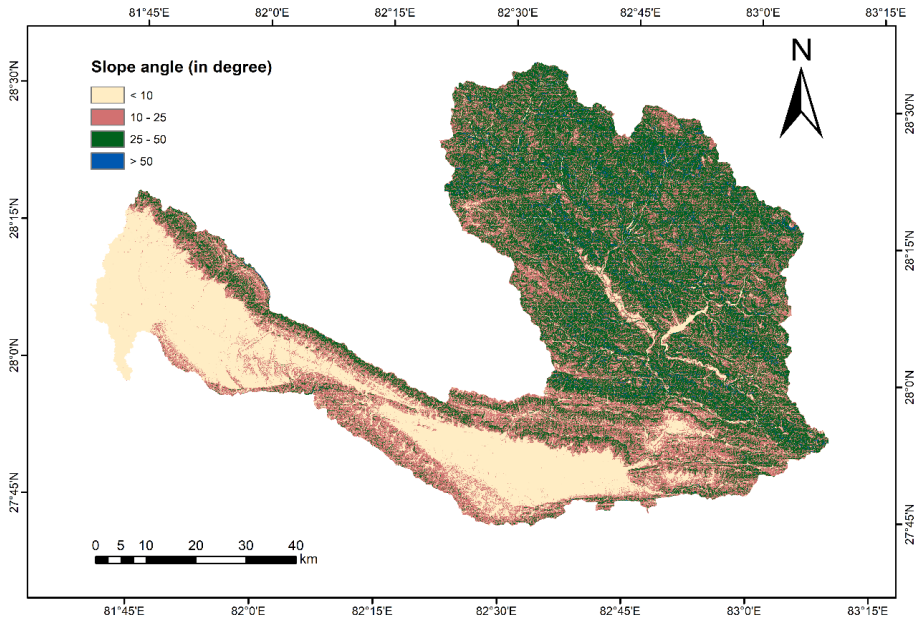**Figure 6.** *Soil Texture map*

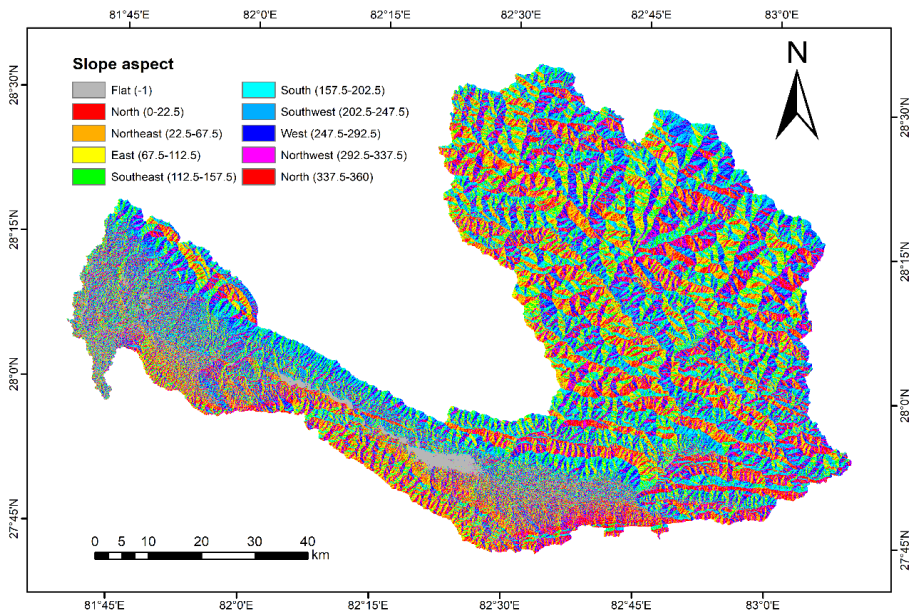**Figure 7.** *Slope angle map*

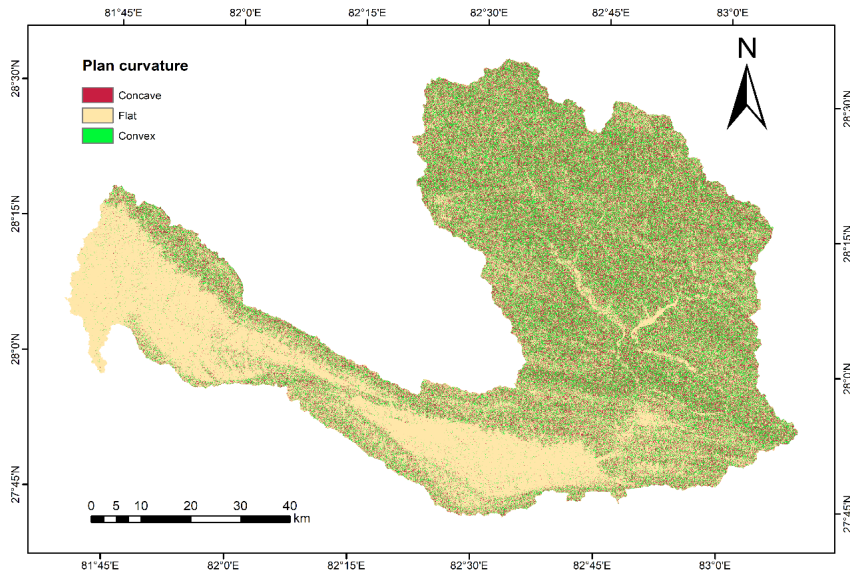**Figure 8.** *Slope Aspect map*

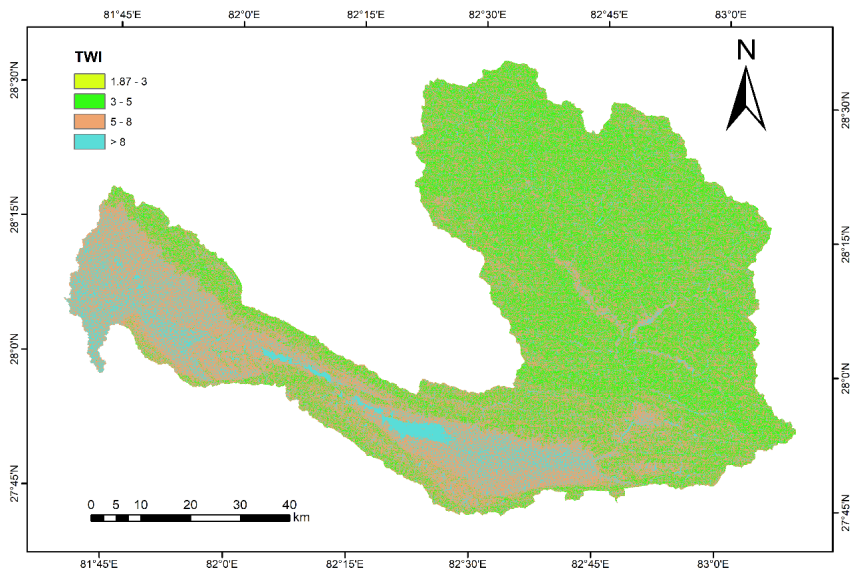**Figure 9.** *Plan curvature map*

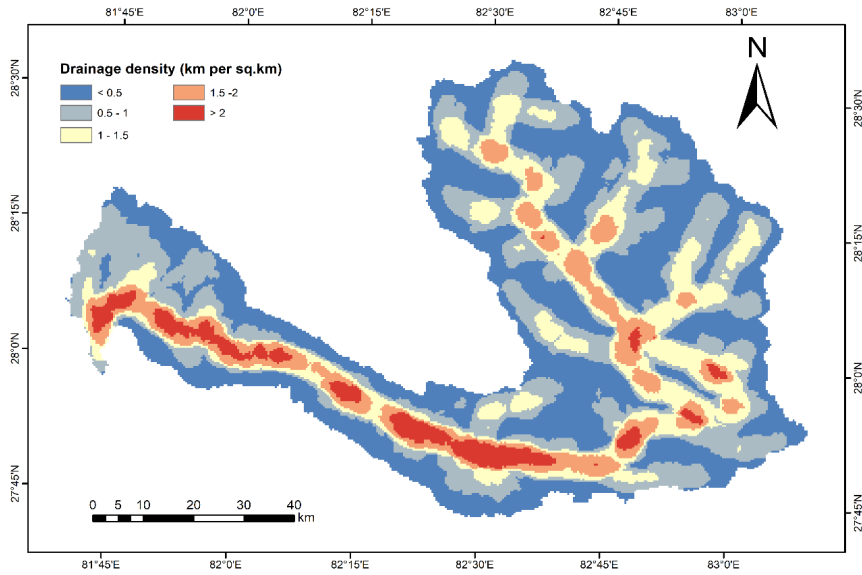**Figure 10.** *Topographic wetness index map*

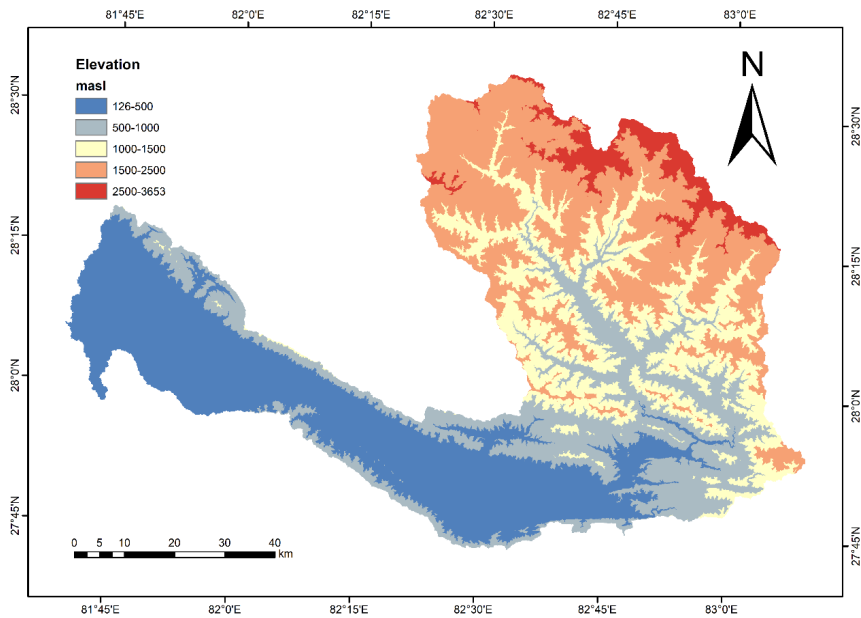**Figure 11.** *Drainage density map*
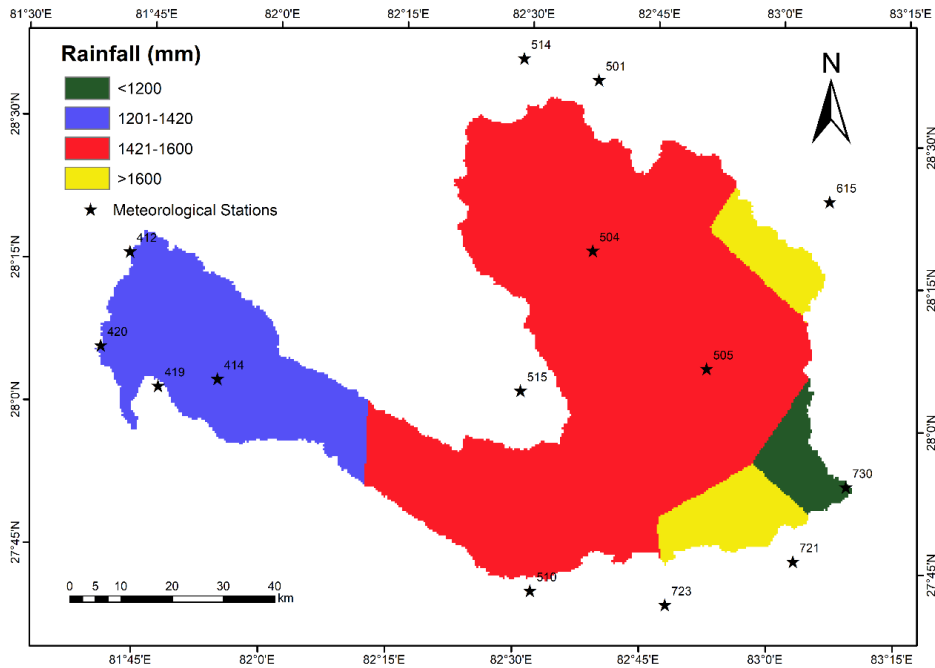

Figure 12. *Elevation Map*

Figure 13. *Rainfall Map*

4.3 Frequency Ratio (FR) Modelling

In the current study, the FR model was chosen from among many bivariate statistical techniques for flood susceptibility mapping. The FR model can be used as a simple geographic assessment tool to assess the stochastic relationship between dependent and independent variables, such as multi-classified maps. (Tehrany et al., 2014) has used this technology to map flood risk. This method is represented by a 'FR index' that depicts the quantitative link between flood incidence and different flood conditioning elements, as represented by Eq. (1):

$$FSI = \sum_{R=1}^{R=n} FR \tag{1}$$

where, FSI represents flood susceptibility index and FR signifies frequency ratio for each flood conditioning factor. n represents number of flood conditioning factors. The FR can be defined as "the ratio of the area where floods occurred in the total study area, it is the ratio of the probabilities of a flood occurrence to a non-occurrence for a given attribute" Eq. (2)(Samanta et al., 2018):

$$FR = \frac{E/F}{M/L} \tag{2}$$

where, E defines the number of pixels with flood for each flood conditioning factor; F represents the total number of floods in the study area; M represents the number of pixels in the class area of the factor; L denotes the number of total pixels in

the study area. The flood susceptibility index in a specific pixel may be calculated by adding the pixel values according to Eq. (1).

5. Results and Discussion

5.1 Outputs from FR Model

FR model was used to establish spatial relationship between flood locations and flood conditioning factors described in Table 2. Their correlation calculated through spatial mapping and analysis is tabulated in Table 3. FR value of one indicates there exists an average interdependence between flood conditioning factors and number of flood events occurring in that location. This implies that if the FR value is greater than one for a particular subclass, there is high probability of flood occurrence. Alternately, FR value lower than one would indicate low risk of flood.

Table 3. FR values for different subclasses of each flood conditioning factor

Class	No of pixels in subclass	Percentage of subclass	No of flood points	Percentage of flood points	Frequency Ratio
Lithology					
Mesozoic intrusive	494744	6.00%	3	3.90%	0.65
Mesozoic and Paleozoic intrusive and metamorphic rocks	1542869	18.71%	16	20.78%	1.11
Neogene sedimentary rocks	2446362	29.67%	19	24.68%	0.83
Undivided Precambrian rocks	2833493	34.36%	22	28.57%	0.83
Quaternary sediments	928682	11.26%	17	22.08%	1.96
Land use					
Water body	473433	0.74%	0	0.00%	0.00
Forest	47864418	75.18%	27	35.06%	0.47
Grassland	72839	0.11%	1	1.30%	11.35
Crops	3489303	5.48%	20	25.97%	4.74
Scrubs/Shrubs	10143694	15.93%	19	24.68%	1.55
Built up area	1260878	1.98%	8	10.39%	5.25
Bare ground	359988	0.57%	2	2.60%	4.59
Distance from River					
<500	731447	8.87%	49	63.64%	7.18
500-2000	1813438	21.99%	18	23.38%	1.06
2000-4000	2007060	24.33%	7	9.09%	0.37
4000-7000	2215172	26.86%	3	3.90%	0.15

7000-10000	1078528	13.08%	0	0.00%	0.00
>10000	402269	4.88%	0	0.00%	0.00
Slope Angle					
<10	2281927	27.67%	43	55.84%	2.02
10-25	2635273	31.96%	20	25.97%	0.81
25-50	3163631	38.36%	14	18.18%	0.47
>50	165640	2.01%	0	0.00%	0.00
Slope Aspect					
Flat	206360	2.50%	8	10.39%	4.15
North	1064031	12.90%	8	10.39%	0.81
Northeast	895479	10.86%	7	9.09%	0.84
East	991491	12.02%	10	12.99%	1.08
Southeast	953500	11.56%	10	12.99%	1.12
South	1075416	13.04%	14	18.18%	1.39
Southwest	1030882	12.50%	6	7.79%	0.62
West	1120942	13.59%	6	7.79%	0.57
Northwest	908370	11.02%	8	10.39%	0.94
Curvature					
Concave	1758293	21.32%	5	6.49%	0.30
Flat	4630807	56.16%	59	76.62%	1.36
Convex	1857371	22.52%	13	16.88%	0.75
Soil Texture					
Colluvial, calcareous	562492	6.82%	3	3.90%	0.57
Fluvial non calcareous	710025	8.61%	16	20.78%	2.41
Fluvial, calcareous	421764	5.12%	12	15.58%	3.05
Gneiss, migmatite	693295	8.41%	0	0.00%	0.00
Quartzite	2885334	35.01%	30	38.96%	1.11
Sandstone, greywacke, arkose	1991918	24.17%	9	11.69%	0.48
slate, phyllite	977335	11.86%	7	9.09%	0.77
Elevation (masl)					
126-500	2572018	31.19%	36	46.75%	1.50
500-1000	1674290	20.30%	27	35.06%	1.73
1000-1500	1544440	18.73%	14	18.18%	0.97
1500-2500	2106226	25.54%	0	0.00%	0.00
2500-3653	349497	4.24%	0	0.00%	0.00
Drainage Density (km per sq. km)					

upto 0.5	3387319	41.07%	3	3.90%	0.09
0.5 - 1	2389952	28.98%	9	11.69%	0.40
1 - 1.5	1337293	16.21%	26	33.77%	2.08
1.5 - 2	767870	9.31%	30	38.96%	4.18
> 2	365480	4.43%	9	11.69%	2.64
TWI					
1.87-3	12988	0.16%	1	1.30%	8.25
3-5	3026980	36.71%	14	18.18%	0.50
5-8	3846409	46.64%	29	37.66%	0.81
>8	1360094	16.49%	33	42.86%	2.60
Rainfall (mm)					
<1200	270204	3.28%	2	2.60%	0.79
1201-1420	1563346	18.96%	18	23.38%	1.23
1421-1600	5725890	69.43%	52	67.53%	0.97
>1600	687213	8.33%	5	6.49%	0.78

It can be inferred from Table 3 that among all lithological subclasses, Quaternary sediments are most susceptible to flood events, with a FR value of 1.96. This lithological formation is mostly prevalent in Terai region of WRRB, as shown in Figure 3. On the other hand, Mesozoic intrusive and Precambrian geology, mostly found in the mid-hills, are less prone to flood events with FR value less than 1. In the case of land use, grasslands are found to be most susceptible to flood although they have the least area coverage. Similarly, built up area and agricultural lands also stand as high flood risk zones while forest and water bodies show the least flood susceptibility. Considering the distance from river, it is quite obvious that the area closer to the river shows great flood risks, with buffer distances less than 500m having FR value 7.18. These findings indicate that flooding occurs primarily near river banks and only occasionally further from rivers. Analysis of slope angle clearly show that area with small slope angles have the highest FR value (2.02 for slope < 10°); thus, suggesting high exposure to flood events. This is due to low runoff and higher retention period of accumulated flood water causing inundation in those area, especially in Terai region as shown in Figure 7. This can also be correlated with the flat slope aspect having the highest FR value (4.15) as well as flat curvature (1.36). To add to that, south facing slopes are more prone to flood occurrences in comparison to the north facing slopes, while other slope aspects and curvatures are relatively less vulnerable.

Furthermore, fluvial calcareous soil texture shows the highest flood vulnerability with FR value of 3.05 followed by fluvial non-calcareous soil texture. These soil textures are mostly abundant in the lower Terai region. Additionally, wider flood plains of river in lower elevation makes these regions more susceptible to frequent flood events. It can also be noted that as the drainage density increases, so does the susceptibility to flooding; with a drainage density range of 1.5-2 km per sq. km showing maximum FR value of 4.18. Other studies have clearly emphasized that the increase in drainage

density corresponds to lowering and quickening of infiltration and surface runoff respectively (Çevik & Topal, 2003). Finally, increase in TWI also indicates high flood risks, with values greater than 8 showing maximum FR value of 2.60. A FR value of 8.25 has been observed in the TWI range of 1.87-3; however, it is due to the small area coverage of this subclass. Finally, for rainfall, it is understood that high rainfall results in high susceptibility to potential floods. However, in our study area, the areas with high rainfall were mostly found to be forests having with high slopes and curvature. Therefore, maximum susceptibility is found to shown by rainfall between 1200-1600mm (around 1), which is mostly along flat regions in the Terai and other habitable and agricultural areas.

Finally, all this flood conditioning factors were combined spatially using Eqn. 3. As depicted in Figure 13, the flood susceptibility has been divided into 4 classes, based on the combined FR value. A higher combined FR value indicates maximum risk of flood events (FR>12.5 classed as Very High), followed by High (10-12.5), Medium (7.5-10) and finally, the low risk zones are classified as low (<7.5) (Samanta et al., 2018). About 16.9 % of the total area of WRRB have been demarcated as high flood prone areas. These areas mostly lie in the lower Terai Basin which are characterized by higher runoff potential, flat slopes, poorly drained soil, lower elevation, and vicinity to the main river. Studies like (Perera et al., 2015) also corroborate with these findings, with previous flood events having been recorded in places like Matehiya, Gangapur, Holiya, Bethani and Phattepur in the Banke district, which lies in the south-western part of WRRB. Moreover, the model output also indicates built up and agricultural areas as highly flood susceptible zones whereas, forest areas show minimal risks, as discussed previously.
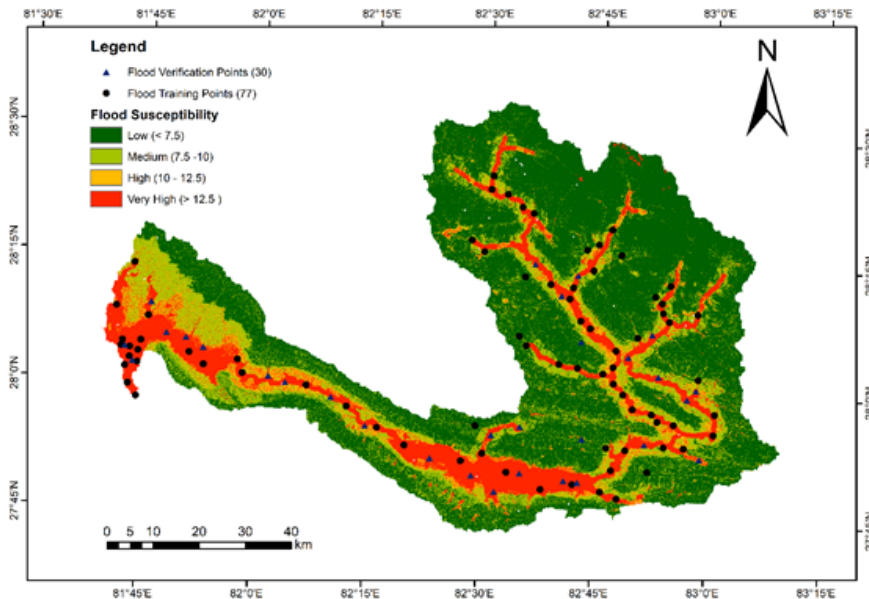

Figure 13. *Flood susceptibility map of the WRRB generated by FR model*

5.2 Validation of FR Model

The main purpose of flood susceptibility study is to identify regions that may be impacted by future floods. Thus, regardless of the model used or methodology adopted, validating the resulting flood susceptibility map critical to delineate the vulnerabilities of stochastic flood occurrences in the future (Chung & Fabbri, 2003). In this study, we used 30 flood locations, which were not used in model training, for validation of the model.

Among different methodologies, Receiver Operating Characteristics (ROC) analysis was adopted as it considered as a reliable method to determine the accuracy of diagnostic tests (Pradhan & Lee, 2009). For every possible cutoff value, this analysis graphically represents false positive and true positive rates on X-axis and Y-axis respectively; the equations of which are described in Eqn. 3-4.

$$X = 1 - specificity = 1 - \frac{TN}{TN + FP} \tag{3}$$

$$Y = sensitivity = \frac{TP}{TP + FN} \tag{4}$$

Where, TN represents True Negative (outcome where model correctly predicts negative class), TP represents True Positive (outcome where model correctly predicts positive class), FP represents False Positive (outcome where model incorrectly predicts positive class), and FN represents False Negative (outcome where model incorrectly predicts negative class).

The area under the curve (AUC) of ROC defines "a prediction model's accuracy by assessing the system's ability to anticipate the proper occurrence or non-occurrence of pre-defined events" (Pourtaghi & Pourghasemi, 2014). The qualitative correlation between AUC and model's prediction accuracy may be described as follows: 50-60% (bad); 60-70% (average); 70-80% (good); 80-90% (very good); and 90-100% (excellent) (Yesilnacar & Topal, 2005). Figure 14 shows the correlation between the ROC curve and the model under different cutoff values. The AUC has been calculated as 80.7%, which implies that the model's prediction accuracy is very good.
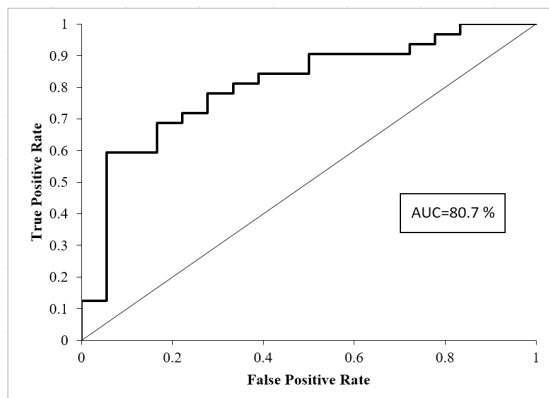

Figure 14. The ROC curve for validation of flood susceptibility map generated by FR model

5.3 Implications under climate change

In the context of climate change, floods have been increasing quite a lot owing to the variations induced in different atmospheric and physical parameters. The uncertainties associated with these climatic variables make long term flood mitigation strategies quite difficult to plan and implement beforehand. However, recent developments have shown that it is possible to project future climate under different scenarios using Global Climatic Models (GCMs) (Chhetri et al., 2021; Mishra et al., 2021). Specifically, the projection of different extreme indices associated with precipitation helps establish a mutual relationship between hydrological extremes (like flood) brought about by them. Therefore, understanding the spatial distribution and temporal patterns of occurrence of precipitation extremes could help devise appropriate flood risk management plans in the future.

Talchabhadel et al. (2021) projected the future precipitation extreme indices in the WRRB, under the scenarios Representative Concentration Pathways (RCP) 4.5 and RCP 8.5 across Near Future (NF): 2025-2049; Mid Future (MF): 2050-2074; and Far Future (FF): 2075-2099. Similarly, Bhattarai et al. (2022) projected climate in this region using latest CMIP6 based climate models. It was found that the heavy precipitation extremes indices (like one-day rainfall, five-day rainfall, 99th percentile rainfall, etc.) were all projected to increase in all future timescales. However, the total annual rainfall did not show much significantly increasing projection. It means that although extreme rainfall occurs in certain periods, periods not receiving rainfall will also increase; thus, vindicating the minimal deviations in the annual rainfall. This intra-variability of rainfall is significant as it suggests the possibility of occurrences of extreme flood events at monsoon while drought may also occur during dry season.

Therefore, the highly susceptible flood areas in the WRRB must be acted upon with appropriate measures to reduce the destructive effects of flood, particularly in climate change context. Further, climatic variability directly affects crop yield; and since people near and around the WRRB directly depend upon agriculture for socio-economic stability, the need to address this compelling situation is a must.

6. Conclusion

FR models can be used effectively to establish relationships between past and future flood events. In this study, we adopted this model to analyze flood susceptible zones in the WRRB. It is crucial to identify different flood conditioning factors, which are spatial inputs to generate a reliable flood model. By integrating spatially analyzed results from 11 flood conditioning factors with 77 flood training points, a flood model was generated and was successfully validated using 30 flood validation points. The lower Terai regions of the WRRB as well as the settlement and agricultural areas were identified as highly susceptible flood zones. Furthermore, areas near the river, particularly those having flat slopes and high drainage density, as well as areas having moderately high rainfall are susceptible to floods as well. With the growing population, change in land use patterns, deforestation, and increase in built-up areas along with the glaring threat of changing climate, it is quite obvious that the risks would only exacerbate in the days to come.

Thus, it is critical for policymakers, technical experts, and concerned authorities in the area to identify necessary measures to mitigate the consequences of extreme flood occurrences, as well as to adopt appropriate watershed management practices in order to preserve the natural environment as well as the lives and property of inhabitants who live in those areas. Such mapping and modelling techniques can be appropriately used in other basins as well, to identify potential flood susceptibility zones and develop appropriate risk management strategies beforehand. The accuracy of these types of models can be further enhanced by adopting advanced tools to prepare precise flood inventory maps. Thus, for a country like Nepal, which frequently experiences extreme flood events resulting in massive human and environmental losses, a national flood inventory map based on detailed surveying, remote sensing and previous flood records is mandatory for better management of flood risks in the future.

Acknowledgment

Declarations

Ethical Approval: Not Applicable
Consent to Participate: Not Applicable
Consent to Publish: Not Applicable
Funding: Not Applicable
Conflict of interests: The authors declare that they have no conflict of interests.
Availability of data and materials: Not Applicable

ANNEX A

Table A: *Description of Stations used in calculation of rainfall*

Meteorological Stations Index	Station Name	Normal_Rainfall (mm)
412	Naubasta	1417.62
414	Baijapur	1150.82
419	Sikta	1453.17
420	Nepalgunj Airport	1467.81
501	Rukumkot	2256.17
504	Libang Gaun	1599.95
505	Bijuwar Tar	1194.7
510	Koilabas	1588.89
514	Musikot(Rukumkot)	2077.14
515	Ghorai (Dang)	1570.06
615	Bobang	2376.29
721	Pattharkot (West)	2182.21
723	Bhagwanpur	1749.07
730	Sitapur (Nepaney)	1895.79

References

Adiat, K. A. N., Nawawi, M. N. M., & Abdullah, K. (2012). Assessing the accuracy of GIS-based elementary multi criteria decision analysis as a spatial prediction tool – A case of predicting potential zones of sustainable groundwater resources. *Journal of Hydrology*, *440–441*, 75–89. https://doi.org/10.1016/J.JHYDROL.2012.03.028

Al-Juaidi, A. E. M., Nassar, A. M., & Al-Juaidi, O. E. M. (2018). Evaluation of flood susceptibility mapping using logistic regression and GIS conditioning factors. *Arabian Journal of Geosciences 2018 11:24*, *11*(24), 1–10. https://doi.org/10.1007/S12517-018-4095-0

Baheti, P. (2022, July). *Train Test Validation Split: How To & Best Practices [2022]*. V7labs.

Bhattarai, T. N., Ghimire, S., Aryal, S., Baaniya, Y., Bhattarai, S., Sharma, S., Bhattarai, P. K., & Pandey, V. P. (2022). Projected changes in hydro-climatic extremes with CMIP6 climate model outputs: a case of rain-fed river systems in Western Nepal. *Stochastic Environmental Research and Risk Assessment*. https://doi.org/10.1007/s00477-022-02312-0

Çevik, E., & Topal, T. (2003). GIS-based landslide susceptibility mapping for a problematic segment of the natural gas pipeline, Hendek (Turkey). *Environmental Geology 2003 44:8*, *44*(8), 949–962. https://doi.org/10.1007/S00254-003-0838-6

Chhetri, R., Pandey, V. P., Talchabhadel, R., & Thapa, B. R. (2021). How do CMIP6 models project changes in precipitation extremes over seasons and locations across the mid hills of Nepal? *Theoretical and Applied Climatology*, *145*(3–4), 1127–1144. https://doi.org/10.1007/s00704-021-03698-7

Chung, C. J. F., & Fabbri, A. G. (2003). Validation of Spatial Prediction Models for Landslide Hazard Mapping. *Natural Hazards 2003 30:3*, *30*(3), 451–472. https://doi.org/10.1023/B:NHAZ.0000007172.62651.2B

Cosby, B. J., Hornberger, G. M., Clapp, R. B., & Ginn, T. R. (1984). A Statistical Exploration of the Relationships of Soil Moisture Characteristics to the Physical Properties of Soils. *Water Resources Research*, 20(6), 682–690. https://doi.org/10.1029/WR020I006P00682

Dangol, S., & Bormudoi, A. (2017). Flood Hazard Mapping and Vulnerability Analysis of Bishnumati River, Nepal. *Journal on Geoinformatics, Nepal*, *14*, 20–24. https://doi.org/10.3126/njg.v14i0.16969

Ercanoglu, M., & Gokceoglu, C. (2002). Assessment of landslide susceptibility for a landslide-prone area (north of Yenice, NW Turkey) by fuzzy approach. *Environmental Geology 2001 41:6*, *41*(6), 720–730. https://doi.org/10.1007/S00254-001-0454-2

Glenn, E. P., Morino, K., Nagler, P. L., Murray, R. S., Pearlstein, S., & Hultine, K. R. (2012). Roles of saltcedar (Tamarix spp.) and capillary rise in salinizing a non-flooding terrace on a flow-regulated desert river. *Journal of Arid Environments*, *79*, 56–65. https://doi.org/10.1016/J.JARIDENV.2011.11.025

IFRC. (2021). *Operation Update Report Nepal : Monsoon floods and landslides*. https://reliefweb.int/report/nepal/nepal-monsoon-floods-and-landslides-operation-update-1-dref-operation-n-mdrnp011

Karki, S., Koirala, M., Pradhan, A. M. S., Thapa, S., Shrestha, A., & Bhattarai, M. (2011). *GIS- Based Flood Hazard Mapping and Vulnerability to Climate Change Assessment: A Case Study from Kankai Watershed, Eastern Nepal*. https://www.researchgate.net/profile/Sunil-Thapa-6/publication/277954182_GIS_Based_Flood_Hazard_Mapping_and_Vulnerability_Assessment_Due_to_Climate_Change_a_case_study_from_Kankai_Watershed_Eastern_Nepal/links/5577163e08aeb6d8c01cdc58/GIS-Based-Flood-Haza

Kia, M. B., Pirasteh, S., Pradhan, B., Mahmud, A. R., Sulaiman, W. N. A., & Moradi, A. (2011). An artificial neural network model for flood simulation using GIS: Johor River Basin, Malaysia. *Environmental Earth Sciences 2011 67:1*, *67*(1), 251–264. https://doi.org/10.1007/S12665-011-1504-Z

Lim, J., & Lee, K. seock. (2017). Investigating flood susceptible areas in inaccessible regions using remote sensing and geographic information systems. *Environmental Monitoring and Assessment 2017 189:3*, *189*(3), 1–13. https://doi.org/10.1007/S10661-017-5811-Z

Liuzzo, L., Sammartano, V., & Freni, G. (2019). Comparison between Different Distributed Methods for Flood Susceptibility Mapping. *Water Resources Management*, *33*(9), 3155–3173. https://doi.org/10.1007/s11269-019-02293-w

Manandhar, B. (2010). *Flood plain analysis and risk assessment of Lothar Khola*. 77. http://www.forestrynepal.org/images/thesis/bikram final_corrected.pdf

Mario Denis, D., Kumar, M., Shankar Srivastava, O., Kumar Srivastava, S., & Kumar, N. (2014). Morphometric analysis of a Semi Urban Watershed, trans Yamuna, draining at Allahabad using Cartosat (DEM) data and GIS. *The International Journal Of Engineering And Science (IJES)* ││. www.theijes.com

Mishra, Y., Babel, M. S., Nakamura, T., & Mishra, B. (2021). Impacts of climate change on irrigation water management in the babai river basin, Nepal. *Hydrology*, *8*(2). https://doi.org/10.3390/HYDROLOGY8020085/S1

Natarajan, L., Usha, T., Gowrappan, M., Palpanabhan Kasthuri, B., Moorthy, P., & Chokkalingam, L. (2021). Flood Susceptibility Analysis in Chennai Corporation Using Frequency Ratio Model. *Journal of the Indian Society of Remote Sensing*, *49*(7), 1533–1543. https://doi.org/10.1007/s12524-021-01331-8

Onuşluel Gül, G. (2013). Estimating flood exposure potentials in Turkish catchments through index-based flood mapping. *Natural Hazards 2013 69:1*, *69*(1), 403–423. https://doi.org/10.1007/S11069-013-0717-8

Pangali Sharma, T. P., Zhang, J., Koju, U. A., Zhang, S., Bai, Y., & Suwal, M. K. (2019). Review of flood disaster studies in Nepal: A remote sensing perspective. *International Journal of Disaster Risk Reduction*, *34*(9), 18–27. https://doi.org/10.1016/j.ijdrr.2018.11.022

Perera, E. D. P., Hiroe, A., Shrestha, D., Fukami, K., Basnyat, D. B., Gautam, S., Hasegawa, A., Uenoyama, T., & Tanaka, S. (2015). Community-based flood damage assessment approach for lower West Rapti River basin in Nepal under the impact of climate change. *Natural Hazards*, *75*(1), 669–699. https://doi.org/10.1007/s11069-014-1339-5

Pourtaghi, Z. S., & Pourghasemi, H. R. (2014). GIS-based groundwater spring potential assessment and mapping in the Birjand Township, southern Khorasan Province, Iran. *Undefined*, *22*(3), 643–662. https://doi.org/10.1007/S10040-013-1089-6

Pradhan, B., & Buchroithner, M. F. (2010). Comparison and Validation of Landslide Susceptibility Maps Using an Artificial Neural Network Model for Three Test Areas in Malaysia. *Environmental and Engineering Geoscience*, *16*(2), 107–126. https://doi.org/10.2113/GSEEGEOSCI.16.2.107

Pradhan, B., & Lee, S. (2009). Regional landslide susceptibility analysis using back-propagation neural network model at Cameron Highland, Malaysia. *Landslides 2009 7:1*, *7*(1), 13–30. https://doi.org/10.1007/S10346-009-0183-2

Rahmati, O., Pourghasemi, H. R., & Zeinivand, H. (2016). Flood susceptibility mapping using frequency ratio and weights-of-evidence models in the Golastan Province, Iran. *Geocarto International*, *31*(1), 42–70. https://doi.org/10.1080/10106049.2015.1041559

Samanta, S., Pal, D. K., & Palsamanta, B. (2018). Flood susceptibility analysis through remote sensing, GIS and frequency ratio model. *Applied Water Science 2018 8:2*, *8*(2), 1–14. https://doi.org/10.1007/S13201-018-0710-1

Shafapour Tehrany, M., Pradhan, B., & Jebur, M. N. (2014). Flood susceptibility mapping using a novel ensemble weights-of-evidence and support vector machine models in GIS. *Journal of Hydrology*, *512*, 332–343. https://doi.org/10.1016/J.JHYDROL.2014.03.008

Shrestha, M. S. (2002). Flood Risk and Vulnerability Mapping Usng Gis : a. *Development*, 1–10.

Sun, D., Yu, Y., & Goldberg, M. D. (2011). Deriving Water Fraction and Flood Maps From MODIS Images Using a Decision Tree Approach. *IEEE Journal of Selected Topics in Applied Earth Observations and Remote Sensing*, *4*(4), 814–825. https://doi.org/10.1109/JSTARS.2011.2125778

Talchabhadel, R., Aryal, A., Kawaike, K., Yamanoi, K., & Nakagawa, H. (2021). A comprehensive analysis of projected changes of extreme precipitation indices in West Rapti River basin, Nepal under changing climate. *International Journal of Climatology*, *41*(S1), E2581–E2599. https://doi.org/10.1002/joc.6866

Talchabhadel, R., Study, A. C., West, O. N., & Watershed, R. (2015). Rainfall Runoff Modelling for Flood. *NEAJ Newsletter*, *Volume 1*,(January), 23–27.

Tehrany, M. S., Lee, M.-J., Pradhan, B., Jebur, M. N., & Lee, S. (2014). Flood susceptibility mapping using integrated bivariate and multivariate statistical models. *Environmental Earth Sciences 2014 72:10*, *72*(10), 4001–4015. https://doi.org/10.1007/S12665-014-3289-3

Uddin, K., & Shrestha, B. (2011). Assessing flood and flood damage using Remote Sensing: a case study from Sunsari, Nepal. *3rd International Conference on Water & Flood Management (ICWFM-2011)*, 293–301. http://www.buet.ac.bd/iwfm/icwfm.php

Wang, Y., Hong, H., Chen, W., Li, S., Pamučar, D., Gigović, L., Drobnjak, S., Bui, D. T., & Duan, H. (2019). A hybrid GIS multi-criteria decision-making method for flood susceptibility mapping at Shangyou, China. *Remote Sensing*, *11*(1). https://doi.org/10.3390/rs11010062

WEPA. (2011). *State of water : Nepal*. http://www.wepa-db.net/policies/state/nepal/state.htm?fbclid=IwAR3fhRSJdnomHYlbvtIONQMhu83kYklLExePTpAcM1aQSJ6IMbbgM8JdlUI

Yesilnacar, E., & Topal, T. (2005). Landslide susceptibility mapping: A comparison of logistic regression and neural networks methods in a medium scale study, Hendek region (Turkey). *Engineering Geology*, *79*(3–4), 251–266. https://doi.org/10.1016/J. ENGGEO.2005.02.002

Yogacharya, K. S., & Gautam, D. K. (2016). Floods in Nepal : Genesis , Magnitude , Frequency and Consequences Floods in Nepal : Genesis , Magnitude , Frequency and Consequences. *Proc. of the International Conference on Hydrology and Climate Change in Mountainous Areas*, *November 2008*, 2016–2030. https://doi.org/10.13140/RG.2.1.2376.8489